Receptor Organization Determines the Limits of Single-Cell Source Location Detection

Sean D. Lawley,[1] Alan E. Lindsay,[2] and Christopher E. Miles[3,*]
[1]Department of Mathematics, University of Utah, Salt Lake City, Utah 84112, USA
[2]Department of Applied and Computational Mathematics and Statistics, University of Notre Dame, South Bend, Indiana 46556, USA
[3]Courant Institute of Mathematical Sciences, New York University, New York, New York 10005, USA

(Received 16 October 2019; accepted 9 June 2020; published 2 July 2020)

Many types of cells require the ability to pinpoint the location of an external stimulus from the arrival of diffusing signaling molecules at cell-surface receptors. How does the organization (number and spatial configuration) of these receptors shape the limit of a cell's ability to infer the source location? In the idealized scenario of a spherical cell, we apply asymptotic analysis to compute splitting probabilities between individual receptors and formulate an information-theoretic framework to quantify the role of receptor organization. Clustered configurations of receptors provide an advantage in detecting sources aligned with the clusters, suggesting a possible multiscale mechanism for single-cell source inference.

DOI: 10.1103/PhysRevLett.125.018102

The ability to pinpoint the location of an external stimulus is critical for a variety of cell types. Canonical examples include eukaryotic gradient-directed cell migration (chemotaxis) [1], directional growth (chemotropism) in growing neurons [2] and yeast [3]. A unifying feature of these systems is that they must infer the spatial location of the external source through the noisy arrivals of diffusing particles to membrane receptors.

The spatial organization of receptors varies between these examples. GABA receptors in nerve cone growth begin relatively uniform on the membrane and dynamically reorganize by clustering receptors toward the source [4]. In budding yeast (*S. cerevisiae*), receptors are known to dynamically cluster towards the direction of a received signal in mate identification [3,5]. In contrast, the receptors in *Dictyostelium* remain uniform throughout the process of identifying a source location. These differences raise the question: what role does receptor clustering play in locating external stimuli?

There has been considerable progress in answering this question. Clustered receptors can provide robustness against noise through rebinding cooperativity [6–10], or by reducing correlation from downstream signals [11]. These observations fit into the broader pursuit of understanding how complex downstream machinery, activated by noisy receptor input, robustly filters shallow gradients [12–20]. Here we study the limits of the most upstream stage: the diffusive arrival of signaling molecules to a fixed configuration of membrane receptors. We find that receptor configuration alone contributes significantly to the quality of signal acquired by the cell.

In this Letter, we establish how receptor organization (number and spatial distribution) shapes the limits of a cell's ability to detect the source location of diffusing particles. Our approach draws from the conceptual model of Berg and Purcell [21] (and later [22]) consisting of a spherical cell with circular absorbing surface sites representing membrane receptors. We employ a matched asymptotic approach to compute the probability a signaling molecule hits a particular receptor [23,24]. Within an information-theoretic framework [25,26], we establish the informational limit of the fully absorbing cell and assess efficiency relative to this limit as a function of the surface fraction and number of receptors. We identify fundamental differences in the information content of clustered receptor configurations, suggesting higher information content in front of clustered receptors. This observation is verified by performing a maximum likelihood inference, showing that a source can be located with smaller average error in front of a cluster of receptors. This suggests a multiscale mechanism for source localization: if a cell can align toward an initial spatial cue (e.g., as observed in budding yeast [3]) with accuracy limited by the spacing between clusters, then it can exploit receptor nonuniformity to pinpoint the location with an accuracy limited by receptor spacing within a cluster.

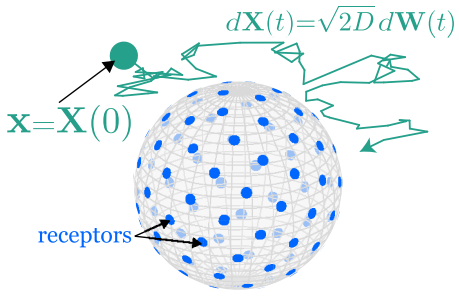

FIG. 1. Model. Diffusing particles are released from a source location $\mathbf{x}$ and either escape to spatial infinity or hit a perfectly absorbing cell-surface receptor.

Model.—Let Ω be the unit sphere with N circular surface receptors of common radius ε. For a diffusing particle originating at $\mathbf{x}$, the splitting probability $p_n(\mathbf{x})$ gives the likelihood of its arrival at the nth receptor, without reaching other receptors or escaping to spatial infinity. The splitting probabilities encode the cell's interaction with the extracellular environment. The probabilities $\{p_n(\mathbf{x})\}_{n=1}^N$ satisfy the mixed boundary value problem

$$\begin{aligned} \Delta p_n &= 0, && \mathbf{x} \in \mathbb{R}^3 \backslash \Omega, \\ p_n &= 1, && \text{on } n\text{th receptor}, \\ p_n &= 0, && \text{on all other receptors}, \\ \partial_\nu p_n &= 0, && \text{elsewhere on cell surface}, \end{aligned} \tag{1}$$

where $\partial_\nu \equiv \hat{\mathbf{n}} \cdot \nabla$ is the normal derivative. The receptor locations are fixed on the surface (cf. Fig. 1) with a general nonoverlapping configuration and centers $\mathcal{Y} = \{\mathbf{y}_1, \ldots, \mathbf{y}_N\}$. Dynamic rearrangement of receptors [3,4] is not explicitly captured in this modeling paradigm, however, how such reorganizations may affect source detection can be inferred by comparing different static configurations. We have derived and validated numerically [27] that as $\varepsilon \to 0$,

$$p_n(\mathbf{x}; \mathcal{Y}) \sim 4\varepsilon G(\mathbf{x}, \mathbf{y}_n) + \frac{4\varepsilon^2}{\pi} \left\{ \left[\frac{3}{2} - \ln(2\varepsilon) \right] G(\mathbf{x}, \mathbf{y}_n) - 4\pi \sum_{\substack{k=1 \\ k \neq n}}^{N} G(\mathbf{y}_n, \mathbf{y}_k) G(\mathbf{x}, \mathbf{y}_k) \right\} + \mathcal{O}(\varepsilon^3). \tag{2}$$

Here $G(\mathbf{x}, \boldsymbol{\xi})$ is the surface Green's function of the Laplacian, exterior to the unit sphere. For $|\boldsymbol{\xi}| = 1$, it is [34]

$$G(\mathbf{x}, \boldsymbol{\xi}) = \frac{1}{2\pi} \left[\frac{1}{|\mathbf{x} - \boldsymbol{\xi}|} - \frac{1}{2} \ln \left(\frac{1 - \mathbf{x} \cdot \boldsymbol{\xi} + |\mathbf{x} - \boldsymbol{\xi}|}{|\mathbf{x}| - \mathbf{x} \cdot \boldsymbol{\xi}} \right) \right].$$

We distinguish between the unconditioned probabilities $p_n(\mathbf{x})$ and the conditioned probabilities

$$q_n(\mathbf{x}; \mathcal{Y}) = \frac{p_n(\mathbf{x}; \mathcal{Y})}{\sum_{k=1}^N p_k(\mathbf{x}; \mathcal{Y})}. \tag{3}$$

The former incorporates the possibility for escape to infinity while the latter only reflects particles which have reached a receptor. By working with the conditioned probabilities, we adopt the biological assumption that the cell has no knowledge about particles that did not arrive at a receptor. The conditional probabilities do not vanish as the receptor radius tends to zero ($\varepsilon \to 0$) and $q_n(\mathbf{x}; \mathcal{Y}) \to G(\mathbf{x}, \mathbf{y}_n) / \sum_{k=1}^N G(\mathbf{x}, \mathbf{y}_k)$.

Consider a fixed, unknown source location $\mathbf{x}$ from which particles are released and denote by c_n the count at the nth receptor. When the number of receptors N and arriving particles $M = \sum_{n=1}^N c_n$ are finite, there is uncertainty in the acquired signal. To quantify this, we first take these quantities to be infinitely large and then consider the case where each is finite.

Case $M = \infty$, $N = \infty$.—To establish the information content in this limit, we consider the arrival distribution to the sphere for a point source at distance $R > 1$ from the cell center. We adopt a coordinate system where the source is located at the north pole, and let $\theta \in [0, \pi)$ and $\phi \in [0, 2\pi)$ denote the arrival location on the sphere. The density describing (θ, ϕ) is equivalent to the classical charge distribution on a conducting sphere induced by a point charge [35–37]

$$f_R(\theta, \phi) = f_R(\theta) = \frac{1 - R^{-2}}{4\pi (1 - 2R^{-1} \cos\theta + R^{-2})^{\frac{3}{2}}} \sin\theta.$$

In the context of cellular decision making [38], we assume that the cell has a prior distribution of each receptor being equally likely to have an arrival of particles; i.e., the cell is initially uninformed about the source location. For the fully absorbing sphere, this yields

$$f_{\text{unif}}(\theta, \phi) = f_{\text{unif}}(\theta) = \frac{1}{4\pi} \sin\theta.$$

The directional information encoded by the arrivals of particles to the surface is therefore a measure of the deviation between the measured and prior distributions. The Kullback-Leibler (KL) divergence, or relative entropy, of q from p is defined by

$$d_{\text{re}}(p \| q) := \int p(x) \ln \left(\frac{p(x)}{q(x)} \right) dx.$$

The relative entropy $d_{\text{re}}(p \| q)$ interpreted in a Bayesian sense computes the amount of information gained revising the belief distribution from q to p. Consequently, the relative entropy from the uniform distribution of arrivals encodes the amount of directional information the cell has. This quantity is found explicitly as a function of R:

$$\begin{aligned} E(R) := d_{\text{re}}(f_R \| f_{\text{unif}}) &= \int_0^{2\pi} \int_0^{\pi} f_R \ln \left(\frac{f_R}{f_{\text{unif}}} \right) d\theta d\phi \\ &= \ln(R) + 3R \coth^{-1}(R) - \frac{1}{2} \ln(R^2 - 1) - 3. \end{aligned}$$

We note that $E(R)$ is positive and monotonically decreasing with intuitive limiting values. As the source approaches the absorbing sphere, $\lim_{R \to 1+} E(R) = \infty$. That is, the noise encoded from diffusion vanishes close to the cell and the arrivals encode the exact direction of the source. However, $E(R) \sim \frac{3}{2} R^{-2}$ as $R \to \infty$, so that for distant sources, diffusion induces more noise in the arrival locations and directional information is reduced.

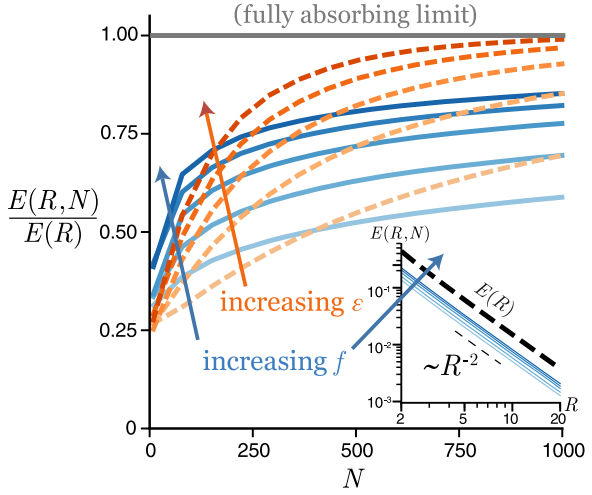

FIG. 2. Directional information with finite number of receptors. Relative entropy from uniform $E(R,N)$ for uniformly spaced receptors as a function of the number of receptors N normalized by the entropy in the fully absorbing sphere limit, $E(R)$. In the red, dashed: receptor radius $\varepsilon = \{1,2,3,4,5\} \times 10^{-2}$, blue, solid: surface fraction $f = \{1, 2.5, 5, 7.5, 10\}\%$ with $R = 5$ fixed. Inset: $E(R,N)$ as a function of R, with $N = 25$ receptors fixed and the same varied surface fractions.

Case $M = \infty$, $N < \infty$.—We now consider a finite number of receptors. From the conditioned probabilities $q_n(\mathbf{x};\mathcal{Y})$ in (3), we define the information gained revising the prior belief from uniform to be the deviation

$$E(R,N) = \sum_{n=1}^{N} \int_{|\mathbf{x}|=R} q_n(\mathbf{x};\mathcal{Y}) \ln\left(\frac{q_n(\mathbf{x};\mathcal{Y})}{1/N}\right) d\mathbf{x}.$$

$E(R,N)$ averages over the angular position of the source. In the calculation for the fully absorbing sphere, the location of the source was chosen arbitrarily due to rotational symmetry. To compare directly to that quantity with explicit receptors, we average over angular positions of the source. Later, we explore the role of angular position relative to receptors in an unaveraged quantity. The probabilities $q_n(\mathbf{x};\mathcal{Y})$ are computed with a numerical solution to (1) for varying source locations and uniformly spaced receptor configurations $\mathcal{Y}$ centered at Fibonacci spiral points [39]. The results of computing $E(R,N)$ for varying number of receptors can be seen in Fig. 2. We first vary the receptor radius ε and see that the resulting behavior is intuitive: as the characteristic distance between receptors decreases, the resolution increases and the fully absorbing sphere serves as a limiting object for finite number of receptors: $E(R,N) \to E(R)$ as $N \to \infty$. Estimates of receptor numbers range from $N \approx 10^4$–10^5 for lymphocytes [40], $N \approx 10^2$ for GABA receptors in neural cone growth [41], and $N \approx 10^4$ in budding yeast [3]. For $N = 1000$ and $\varepsilon = 0.05$, the largest values in the figure, the surface fraction coverage $f = \varepsilon^2 N/4$ is approximately $f \approx 70\%$ and the information content is effectively at the limit of the fully absorbing sphere.

Is this effect due to having more receptors or just a byproduct of increasing the absorbing surface area? We instead vary f (setting $\varepsilon = \sqrt{4f/N}$) and observe that the information content still increases as a function of N. In the case of 1% surface fraction coverage by $N = 1000$ receptors, the directional information content is over 50% of the fully absorbing limit [42]. This surprising result is analogous to the Berg and Purcell flux dependence on the absorbing surface perimeter. The probabilities q_n are influenced by arrivals to other receptors, the rate at which is controlled by the flux, meaning again the perimeter is the factor that influences the rate at which information is gained. In the inset of Fig. 2, we see $E(R,N) \sim R^{-2}$ as $R \to \infty$ alongside the perfectly absorbing limit.

Clustered receptor configurations.—We have so far examined how a finite number of uniformly distributed receptors approaches the fully absorbing sphere limit. Receptor clustering reduces the total flux to the receptors [44], but it remains to determine the effect on directional sensing. The relative entropy in this case is the nonaveraged quantity

$$E(\mathbf{x};\mathcal{Y}) = \sum_{n=1}^{N} q_n(\mathbf{x};\mathcal{Y}) \ln\left(\frac{q_n(\mathbf{x};\mathcal{Y})}{1/N}\right). \tag{4}$$

For a given source location $\mathbf{x}$ and receptor configuration $\mathcal{Y}$, this measure should be interpreted as a prior distribution of uniform probabilities across receptors, which is not necessarily equivalent to any particular distribution of $\mathbf{x}$, the quantity being estimated. See [45] for a discussion of priors in direction sensing.

Let $\mathcal{Y}_{\text{clust}}$ and $\mathcal{Y}_{\text{unif}}$ denote clustered and uniform receptor configurations (Fig. 3). Clustered configurations are formed by placing receptors in a spherical cap and copying across the sphere at Fibonacci spiral points. For these configurations, the relative entropy (with respect to uniform probabilities) is computed using the asymptotic result (2) and shown in Fig. 3. The asymptotic result allows for rapid evaluation of these probabilities at a large number of source locations.

In Fig. 3, the directional relative entropy appears to be heterogeneous in space for $\mathcal{Y}_{\text{clust}}$ but directionally uniform for $\mathcal{Y}_{\text{unif}}$. The difference $E(\mathbf{x};\mathcal{Y}_{\text{clust}}) - E(\mathbf{x};\mathcal{Y}_{\text{unif}})$ (Fig. 3, right column) indicates that directional entropy in front of a cluster is higher than that of the uniform configuration, and this difference diminishes as source distance increases. This implies that informational content is richer for the clustered configuration when particles are arriving from sources in front of the cluster.

To explore further, we compute in Fig. 4 the difference in entropy both in front of a cluster and averaged over possible source locations [i.e., $E(R\mathbf{e}_x;\mathcal{Y})$ and $\int_{|\mathbf{x}|=R} E(\mathbf{x};\mathcal{Y}) d\mathbf{x}$]. The results are shown for 45 total receptors and source

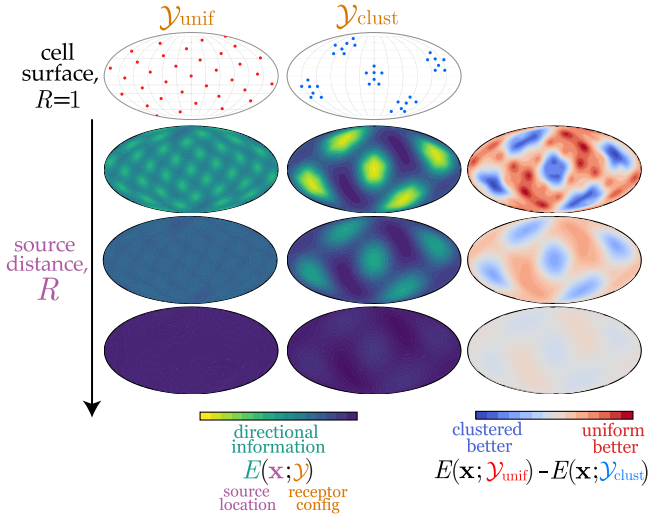

FIG. 3. Relative entropy for two receptor configurations. Left and center columns: the directional entropy (4) as a function of the source location for each configuration and $R = \{1.25, 1.75, 2.5\}$. Right column: the difference between the two entropies. At smaller R values, clustered configurations can receive more directional information. This difference diminishes at large R values suggesting receptor organization plays a negligible role when locating distant sources.

distances $R = 2$, 4. In front of a cluster, nonuniform configurations have higher entropy levels, but on average, perform worse. The benefits of clustering become diminished as the source location becomes farther away or the configuration becomes less clustered. The resolution is therefore determined by the spacing between receptors. Thus, smaller receptor spacing within a cluster can resolve finer detail. Expectedly, as the source location moves away,

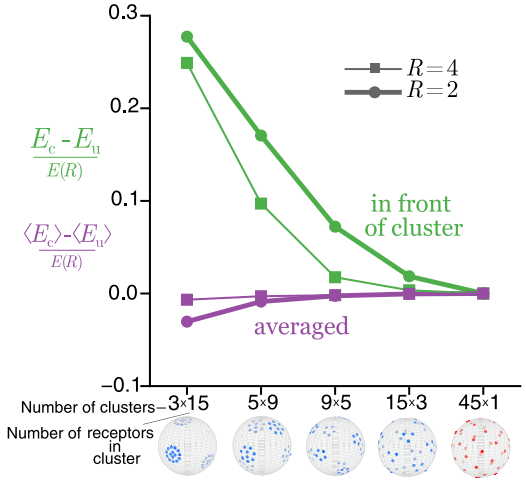

FIG. 4. Comparison of entropies for clustered and uniform receptor configurations. Difference in entropy is computed in front of the cluster (green) and averaged over source locations (purple). Clustered configurations have higher relative entropy in front of clusters but lower on average, with this effect most magnified close to the cell.

the noise from diffusion makes both distributions converge to uniform probabilities and the difference vanishes.

Case $M < \infty$, $N < \infty$.—For infinitely many incident particles ($M = \infty$), the q_n are discerned exactly. How does source inference operate given a noisy sample formed by finite arrivals? The probabilities of arrival at each receptor are multinomial (dependent on $\mathbf{x}$) with likelihood

$$L(\mathbf{x};\mathcal{Y}) = \sum_{n=1}^{N} \frac{c_n}{M} \ln[q_n(\mathbf{x},\mathcal{Y})].$$

The maximum likelihood estimate (MLE) of the source is

$$\hat{\mathbf{x}}_{\text{MLE}} = \arg\max_{\mathbf{x}} L\,(\mathbf{x};\mathcal{Y}). \tag{5}$$

We use this inference scheme only as a statistical abstraction to quantify the limits of uncertainty in the system. Cellular mechanisms for MLE-based [46] or Bayesian [47] inference have been proposed but are fundamentally downstream of diffusive arrivals and beyond the scope of this Letter. Relative entropy and Fisher information (the standard error of MLE) are related [48] so we expect the previous results about relative entropy to inform the error in

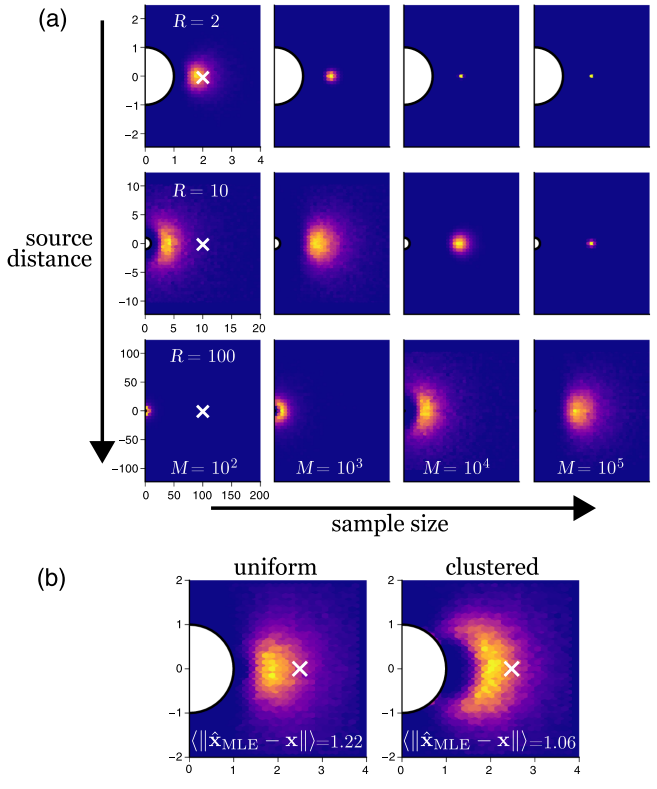

FIG. 5. Frequency of maximum likelihood estimated locations. (a) For varying source locations $\mathbf{x}$ at a distance R (from the center of the cell) and sample sizes M, frequencies of MLE estimated locations (5) for uniform receptor covering. (b) estimated locations for the configurations of receptors shown in Fig. 3. Colors correspond to relative frequency of estimated location.

the MLE estimate. In Fig. 5(a), we vary the source location $\mathbf{x} = (R,0,0)$ for $R = 2, 10, 100$ and $M = 10^2, 10^3, 10^4, 10^5$. The receptor configuration remains the uniform configuration in Fig. 3. For each trial, we compute the MLE estimate numerically from (5) with $z = 0$ fixed and plot the frequency of results. The error $\langle \|\hat{\mathbf{x}}_{\mathrm{MLE}} - \mathbf{x}\| \rangle$ scales $\sim M^{-1/2}$, as predicted by the central limit theorem but also as $\sim R^{-2}$ [27], in accordance with the relative entropy results in the $M = \infty$ case. To verify the claim in Fig. 3 that certain source locations may be better detected by a clustered configuration, we fixed the source at $\mathbf{x} = (2.5, 0, 0)$ and took $M = 50$ particles. The frequency of predicted locations, shown in Fig. 5(b), yields a lower mean error for the clustered configuration than that of the uniform.

Discussion.—We have examined the role of receptor organization on detection of external stimuli. We demonstrate that a cell can operate near theoretical limits with a finite number of receptors and noisy arrival data. When receptors are not uniformly spaced, the information content is larger in front of clusters suggesting that resolution is limited by receptor spacing. A cell with clustered receptors can potentially benefit by forming a crude estimate and aligning itself in that direction.

Altogether, our results reinforce the notion that cells must balance trade-offs between directional signal coverage and robustness as seen in other work [8–11]. However, we emphasize that the only mechanism by which receptors are interacting in our model is through binding competition, as no downstream signaling or rebinding are included. Understanding the interplay between receptor organization and downstream signaling mechanisms is a natural direction for future investigations. Finally, it would be interesting to study the relative entropy of physiological or dynamical cluster configurations (e.g., [8]) compared to the synthetic ones utilized here. Our Letter suggests the spatial organization of membrane bound receptors plays a crucial role in cellular scale directional sensing and decision making.

Two authors are supported by the NSF (S. D. L. by Grants No. DMS-1944574, No. DMS-1814832, and No. DMS-1148230, A. E. L. by Grant No. DMS-1815216). Support and resources from The Convergence Accelerator Team program at the NSF-Simons Center for Multiscale Cell Research, funded by NSF Grant No. DMS-1763272 and a grant from the Simons Foundation (Grant No. 594598, Q. N.), and the AMS Mathematical Research Communities program are gratefully acknowledged.

*christopher.miles@cims.nyu.edu

[1] A. Levchenko and P. A. Iglesias, Biophys. J. **82**, 50 (2002).
[2] G. J. Goodhill, Trends Neurosci. **39**, 202 (2016).
[3] A. Ismael, W. Tian, N. Waszczak, X. Wang, Y. Cao, D. Suchkov, E. Bar, M. V. Metodiev, J. Liang, R. A. Arkowitz, and D. E. Stone, Sci. Signal. **9**, ra38 (2016).
[4] C. Bouzigues, M. Morel, A. Triller, and M. Dahan, Proc. Natl. Acad. Sci. U.S.A. **104**, 11251 (2007).
[5] R. Yonashiro, A. Sugiura, M. Miyachi, T. Fukuda, N. Matsushita, R. Inatome, Y. Ogata, T. Suzuki, N. Dohmae, and S. Yanagi, Mol. Biol. Cell **20**, 4524 (2009).
[6] D. Bray, M. D. Levin, and C. J. Morton-Firth, Nature (London) **393**, 85 (1998).
[7] B. R. Caré and H. A. Soula, BMC Syst. Biol. **5**, 48 (2011) .
[8] G. Iyengar and M. Rao, Proc. Natl. Acad. Sci. U.S.A. **111**, 12402 (2014).
[9] H. Nguyen, P. Dayan, and G. J. Goodhill, J. Theor. Biol. **360**, 95 (2014).
[10] P. Recouvreux and P. F. Lenne, Curr. Opin. Cell Biol. **38**, 18 (2016).
[11] A. Mugler, F. Tostevin, and P. R. Ten Wolde, Proc. Natl. Acad. Sci. U.S.A. **110**, 5927 (2013).
[12] L. Song, S. M. Nadkarni, H. U. Bödeker, C. Beta, A. Bae, C. Franck, W. J. Rappel, W. F. Loomis, and E. Bodenschatz, Eur. J. Cell Biol. **85**, 981 (2006).
[13] P. J. Van Haastert and M. Postmay, Biophys. J. **93**, 1787 (2007).
[14] F. Tostevin, P. R. Ten Wolde, and M. Howard, PLoS Comput. Biol. **3**, e78 (2007).
[15] W. J. Rappel and H. Levine, Phys. Rev. Lett. **100**, 228101 (2008).
[16] R. G. Endres and N. S. Wingreen, Proc. Natl. Acad. Sci. U.S.A. **105**, 15749 (2008).
[17] R. G. Endres and N. S. Wingreen, Prog. Biophys. Molec. Biol. **100**, 33 (2009).
[18] G. Aquino, L. Tweedy, D. Heinrich, and R. G. Endres, Sci. Rep. **4**, 5688 (2015).
[19] T. Strünker, L. Alvarez, and U. B. Kaupp, Curr. Opin. Neurobiol. **34**, 110 (2015).
[20] V. Lakhani and T. C. Elston, PLoS Comput. Biol. **13**, e1005386 (2017).
[21] H. C. Berg and E. M. Purcell, Biophys. J. **20**, 193 (1977).
[22] W. Bialek and S. Setayeshgar, Proc. Natl. Acad. Sci. U.S.A. **102**, 10040 (2005).
[23] U. Dobramysl and D. Holcman, Sci. Rep. **8**, 941 (2018).
[24] U. Dobramysl and D. Holcman, J. Comput. Phys. **355**, 22 (2018).
[25] B. W. Andrews and P. A. Iglesias, PLoS Comput. Biol. **3**, e153 (2007).
[26] J. M. Kimmel, R. M. Salter, and P. J. Thomas, Adv. Neural Inf. Process. Syst. **19**, 705 (2007), https://papers.nips.cc/paper/2995-an-information-theoretic-framework-for-eukaryotic-gradient-sensing.
[27] See Supplemental Material at http://link.aps.org/supplemental/10.1103/PhysRevLett.125.018102 for details on the asymptotic splitting probabilities and source location inference simulations, which includes Refs. [28–33].
[28] I. N. Sneddon, *Elements of Partial Differential Equations* (McGraw-Hill Book Company, Inc., New York, 1957).
[29] I. N. Sneddon, *Mixed Boundary Value Problems in Potential Theory* (North-Holland, Amsterdam, 1966).
[30] D. G. Duffy, *Mixed Boundary Value Problems* (Chapman and Hall/CRC, Boca Raton, 2008).

[31] P. Novák and J. Novák, Proc. SPIE Int. Soc. Opt. Eng. **8789**, 878913 (2013).
[32] A. J. Bernoff and A. E. Lindsay, SIAM J. Appl. Math. **78**, 266 (2018).
[33] Á. González, Math. Geosci. **42**, 49 (2009).
[34] I. M. Nemenman and A. S. Silbergleit, J. Appl. Phys. **86**, 614 (1999).
[35] A. Tikhonov and A. Samarskii, *Equations of Mathematical Physics* (Pergamon Press Ltd., Oxford, 1963).
[36] B. A. Luty, J. A. Mccammon, and H. X. Zhou, J. Chem. Phys. **97**, 5682 (1992).
[37] C. Hwang and M. Mascagni, J. Appl. Phys. **95**, 3798 (2004).
[38] C. G. Bowsher and P. S. Swain, Curr. Opin. Biotechnol. **28**, 149 (2014).
[39] R. Swinbank and R. J. Purser, Q. J. R. Meteorol. Soc. **132**, 1769 (2006).
[40] A. S. Perelson and G. Weisbuch, Rev. Mod. Phys. **69**, 1219 (1997).
[41] C. Bouzigues, D. Holcman, and M. Dahan, PLoS One **5**, e9243 (2010).
[42] We expect that for a large enough N, the curves for fixed f would approach the limit. This could be investigated with fast numerical schemes such as Ref. [43].
[43] J. Kaye and L. Greengard, J. Comput. Phys. **5** 100047 (2020).
[44] A. E. Lindsay, A. J. Bernoff, and M. J. Ward, Multiscale Model. Simul. **15**, 74 (2017).
[45] B. Hu, W. Chen, H. Levine, and W. J. Rappel, J. Stat. Phys. **142**, 1167 (2011).
[46] R. G. Endres and N. S. Wingreen, Phys. Rev. Lett. **103**, 158101 (2009).
[47] T. Mora and I. Nemenman, Phys. Rev. Lett. **123**, 198101 (2019).
[48] C. Gourieroux and A. Monfort, *Statistics and Econometric Models*, 1st ed. (Cambridge University Press, Cambridge, England, 1995), p. 524.